sciendo

Polish Journal of Medical Physics and Engineering
The Journal of Polish Society of Medical Physics
ISSN 1898-0309, doi: 10.2478/pjmpe-2018-0024

December 2018
Vol 24, Issue 4

Scientific Paper

Implementation of compensator-based intensity modulated radiotherapy with a conventional telecobalt machine using missing tissue approach

Samuel N. A. TAGOE[1,2,a], Samuel Y. MENSAH[2], John J. FLETCHER[3]

[1]*National Centre for Radiotherapy and Nuclear Medicine, Korle Bu Teaching Hospital, Accra, Ghana*
[2]*Department of Physics, School of Physical Sciences, College of Agriculture and Natural Sciences, University of Cape Coast, Cape Coast, Ghana*
[3]*Department of Applied Physics, University for Development Studies, Navrongo Campus, Navrongo, Ghana.*
[a]*E-mail address: s.tagoe@kbth.gov.gh*

(received 22 April 2018; revised 14 June 2018; accepted 7 August 2018)

Abstract

Objectives: The present study aimed to generate intensity-modulated beams with compensators for a conventional telecobalt machine, based on dose distributions generated with a treatment planning system (TPS) performing forward planning, and cannot directly simulate a compensator.

Materials and Methods: The following materials were selected for compensator construction: Brass, Copper and Perspex (PMMA). Boluses with varying thicknesses across the surface of a tissue-equivalent phantom were used to achieve beam intensity modulations during treatment planning with the TPS. Beam data measured for specific treatment parameters in a full scatter water phantom with a 0.125 cc cylindrical ionization chamber, with a particular compensator material in the path of beams from the telecobalt machine, and that without the compensator but the heights of water above the detector adjusted to get the same detector readings as before, were used to develop and propose a semi-empirical equation for converting a bolus thickness to compensator material thickness, such that any point within the phantom would receive the planned dose. Once the dimensions of a compensator had been determined, the compensator was constructed using the cubic pile method. The treatment plans generated with the TPS were replicated on the telecobalt machine with a bolus within each beam represented with its corresponding compensator mounted on the accessory holder of the telecobalt machine.

Results: Dose distributions measured in the tissue-equivalent phantom with calibrated Gafchromic EBT2 films for compensators constructed based on the proposed approach, were comparable to those of the TPS with deviation less than or equal to ± 3% (mean of 2.29 ± 0.61%) of the measured doses, with resultant confidence limit value of 3.21.

Conclusion: The use of the proposed approach for clinical application is recommended, and could facilitate the generation of intensity-modulated beams with limited resources using the missing tissue approach rendering encouraging results.

Key words: telecobalt machine; bolus; compensator; Gafchromic film; intensity modulated.

Introduction

Dose distribution within a patient has been found to be the most reliable and verifiable quantity that links treatment parameters of any radiotherapy treatment technique to treatment outcome [1,2]. It is therefore imperative to choose irradiation geometries that will maximise radiation dose to the tumour volume while concurrently minimizing doses to normal tissues in close proximity to tumour volume during external beam radiation therapy (EBRT) to achieve favourable treatment outcome. The dose distribution is influenced very much by skin surface contour (body shape) and tissue inhomogeneities. Influence of body shape on dose distribution may be diminished by using individually designed bolus [3]. Use of a bolus leads to an undesirable skin doses, which can be minimized by moving the bolus distance of 15-20 cm from the skin while still achieving the purpose of the bolus [3]. By virtue of the position of the bolus and its objective, the bolus is referred to as missing tissue compensator [3]. Owing to the position of the compensator, it may be composed of any material.

The aforementioned factors (skin topography and tissue inhomogeneity) coupled with the often complex shapes of tumours will require or necessitate the modulation of the fluence distribution across beams from conventional teletherapy machines. This has culminated in the introduction of Intensity Modulated Radiotherapy (IMRT), where extensively intensity modulated (IM) beams are used [2]. IMRT is becoming more widespread, and it is usually

implemented using linear accelerator equipped with multileaf collimator (MLC) to facilitate the creation of variable fluence distributions within an irradiated region of a patient during EBRT. Desired dose distributions within the patient prior to treatment delivery are simulated with a treatment planning system (TPS) that can perform inverse planning or a forward planning TPS with direct aperture optimization (DAO) software [4,5]. These treatment planning approaches help in the realization of beam intensity maps to be replicated with the sequential movements of the various leaves of the MLC system or by individual compensators each having varying thicknesses across a beam [2]. Realization of fluence distribution across beams prior to treatment delivery is paramount to any IMRT delivery technique (or generation of IM beams). Delivering IMRT with compensators is receiving renewed interest from the radiotherapy community due its static nature and simplicity [2]. With reference to the above, some vendors of treatment planning systems are incorporating features to facilitate easy implementation of compensator-based IMRT; referred to as solid IMRT. The Pre-requirements for modern day IMRT are capital intensity and may be out of reach of many developing countries [6,7].

Alternative approach of generating IM beams with customized compensators for a radiotherapy facility using a conventional telecobalt machine for EBRT and a forward planning TPS, that cannot generate intensity maps of beams as well as simulate directly a compensator, is being present. In the present study, boluses of varying thicknesses placed on the surface of a tissue equivalent phantom are used to provide beam intensity modulations during treatment planning (simulation) with the forward planning TPS. The generated treatment plans are replicated on the telecobalt machine with compensators composed of medium density materials placed certain distances from the phantom such that dose distributions within the phantom are the same as planned. Procedures adopted to obtain the physical dimensions of a compensator to provide desired dose distribution within a patient are also presented.

Materials

The following equipment were used to facilitate the development of the proposed method for generating IM beams for a telecobalt machine:

- Blue Phantom^2 three dimensional water phantom (IBA Dosimetry GmbH, Germany)
- Small stationary water phantom (T41014; PTW-Freiburg, Germany)
- Solid water phantom (T2967; PTW-Freiburg, Germany)
- 0.125 cc Semiflex cylindrical ionization chamber (TW31010; PTW-Freiburg, Germany)
- 0.60 cc Farmer type cylindrical ionization chamber (TW 30013; PTW-Freiburg, Germany)
- UNIDOS electrometer (T10002- 020427; PTW-Freiburg, Germany)
- ScanMaker 9800XL plus flatbed scanner (Microtek, USA)
- Pack of EBT2 Gafchromic films (lot # 08221302; International Specialty products, USA)
- Prowess Panther treatment planning system (version 4.6; Prowess Inc., USA)

Beam intensity modulations based on the proposed approach were performed for an Equinox 100 cobalt 60 teletherapy machine (Best Theratronics, Canada). The telecobalt machine was manufactured in April, 2013. The treatment head of the telecobalt machine is mounted isocentrically with source axial distance (SAD) of 100 cm. In the treatment head is contained a double encapsulated cobalt 60 source having initial total source activity of 399.0 TBq (measured on August 1, 2013, by source manufacturer, Nordion Inc., Canada). This gives the teletherapy machine a reference beam output in water at the depth of maximum dose (0.5 cm) of 189.49 cGy/min (on December 12, 2013), measured after installation of the telecobalt machine, based on International Atomic Energy Agency (IAEA) technical series report (TRS) 398 protocol [8]. Percentage depth dose for the reference field size of 10 cm x 10 cm for a depth of 10 cm in water (PDD10), which is used as a beam quality specifier for megavoltage beams [9], is 58.36 % for the telecobalt machine. High activity encapsulated cobalt 60 source within the treatment head of the teletherapy machine has a diameter of 2 cm and length of 4 cm, and is classified as C-146 teletherapy source capsules by Canadian Nuclear Safety Commission [10]. The source is embedded in a source drawer mechanism which uses a pneumatic system to bring the source in and out of treatment position. The circular end of the source is towards the direction of propagation of beams from the telecobalt machine. Within the treatment head are asymmetrical collimators that allow the jaws, which define the shape of the beam to move independently of each other, providing more freedom in treatment planning. Attached to the collimator system is an accessory holder with block tray code interlock to prevent the use of a wrong accessory for treatment. The distance of radiation source to the accessory holder (or block tray) is 59.3 cm. The telecobalt machine is configured to have features of a modern medical linear accelerator with the exception of a multileaf collimator system and an electronic portal imager. The field size that can be set on the machine ranges from 1 x 1 to 43 x 43 cm^2 (defined at the machine isocenter). The machine features a new Motorized Wedge (MW) system, which allows one to treat with any wedge angle ranging from 0 to 60 degrees. This is made possible with a fixed 60 degrees physical wedge permanently positioned in the treatment head of the machine, which can be brought automatically in and out of the path of the radiation beam during treatment delivery, such that combinations of time weighted beams with and without the wedge filter create the dosimetric effects of the required wedge. A picture of the telecobalt machine showing setup for the acquisition of necessary beam data to facilitate the development of the proposed approach for beam intensity modulation is shown in **Figure 1**.

The following materials each in the form of both plates (or slabs; having dimensions of 22 cm x 22 cm) and cubic blocks, having varying thicknesses, were selected for compensator construction based on the proposed approach: Copper, Brass and Perspex. Criteria for the selection of a material were as follows: the material should be of a medium density, non-corrosive, environmentally friend, easy to machine into required shape and must retain the shape once formed, must be readily available and of relatively low cost. The first criterion takes into consideration the energy of the beam to be modulated and the level of modulation required. Also, uncertainties in determining the required thickness of a compensator to apply would translate to relatively low discrepancies in the expected doses within a patient if a medium density material is used. The remaining criteria precinct on physical properties or characteristics of the compensator material.

Methods

Prior to the experimental measurements to facilitate the development of the proposed method, radiological properties relative to those of water of the various selected compensator materials were measured to ensure reproducibility of the proposed method. For each of the selected materials, linear attenuation coefficient was measured in air with beams from the telecobalt machine. Each beam had a field size of 10 cm x 10 cm, and source to detector distance (SDD) of 100 cm was used. The 0.125 cc ionization chamber having its build-up cap (PMMA, thickness of 3 mm; provided by the manufacturer) on was used for the linear attenuation coefficient measurements. For the measurement of linear attenuation coefficient of water, a specialized graduated water tank (see **Figure 2**) that could be mounted on the accessories holder of the teletherapy machine, to hold varying volumes of water in the path of beams from the telecobalt machine, was fabricated from 0.6 cm Perspex (acrylic) sheets. The thicknesses of the various compensator materials used for the measurements ranged from: 0 to 29.61 mm (increment of 3.29 mm), 0 to 18 mm (increment of 3 mm), and 0 to 72.00 mm (increment of 8 mm) for copper, brass and Perspex, respectively. The 22 cm x 22 cm compensator material plates (or slabs) were used for the attenuation measurements. For measurements with water, the height of water within the fabricated tank was adjusted from 0 to 12 cm (increment of 2 cm). Densities of the various compensator materials were also determined. For a specific compensator material, the density was calculated from the ratio of the mass (measured with a digital chemical balance) to the volume (determined from measured physical dimensions of the compensator material with digital caliper) of the compensator material. Since Compton interaction predominates at the megavoltage energy range in use for therapy, it would be prudent to express the linear attenuation coefficient of a compensator material in terms of mass attenuation coefficient to remove the dependence of density of the compensator material. The mass attenuation coefficient, μ_m of an absorber for a particular beam quality is defined as:

$$\mu_m = \frac{\mu}{\rho} \qquad \text{Eq. 1}$$

where μ and ρ are the linear attenuation coefficient of the absorber measured with the required beam quality and the density of the absorber respectively.

Figure 1. Telecobalt machine with beam measuring equipment (Blue Phantom^2 water phantom) in the path of beam.

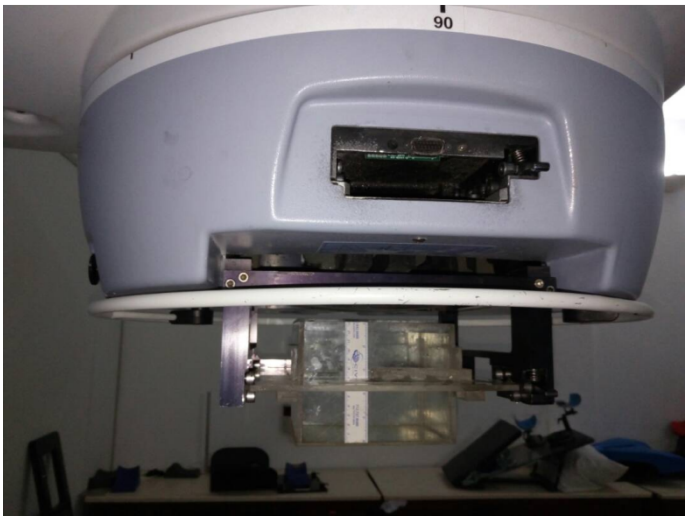

Figure 2. Locally fabricated water tank mounted on the accessories holder of telecobalt machine during measurement of attenuation coefficient of water.

The relationship between the thickness, x_b, of an applied bolus on the surface of a tissue-equivalent phantom and that of the representing compensator material, x_c, placed at certain distance from the surface of the phantom along a particular ray line (or beamlet), such that dose at any point within the phantom remains the same, was obtained using the semi-empirical formula proposed by Tagoe *et al*, which is given as [1]:

$$x_c = x_b T_\rho f_r f_d \quad \text{Eq. 2}$$

where T_ρ is the appropriate thickness density ratio of a particular compensator material relative to that of water measured for a specified reference conditions (field size of 10 cm x 10 cm and treatment depth of 5 cm, employing isocentric irradiation technique); f_d and f_r are correction factors introduced to account for the effects of treatment depth and field size respectively. The various terms in **Equation 2** were obtained by measuring the output of the telecobalt machine in a full scatter water phantom for specific field size and treatment depth with a particular thickness of a compensator material in the path of the beam, and then repeating the measurement without the compensator, but the height of water above the detector adjusted to obtain the same detector reading as before with the compensator. These measurements were repeated for various field sizes and treatment depths, and the readings obtained normalized to those of the reference conditions to determine expressions for the correction factors introduced through correlation analyses. The field size used ranged from 3 cm x 3 cm to 35 cm x 35 cm, and that of treatment depth ranged from 0.5 to 18 cm. Determination of expression for the thickness density ratio, T_ρ, was achieved by using varying thicknesses of a particular compensator material. For the various compensator materials, the thickness ranges were similar to those used for the linear attenuation coefficient measurements. Also, the dimensions of the various compensator materials employed in the various measurements to facilitate the development the semi-empirical formula (**Equation 2**) were similar to those used for the attenuation coefficient measurements. All beam data to facilitate the development of the proposed approach were acquired with the three dimensional water phantom which was connected to a laptop having the OmniPro-Accept 7 software of the same manufacturer required for the running of the water phantom. The 0.125 cc ionization chamber which was connected to the UNIDOS electrometer, was used for the measurements in the water phantom. Details of the measurement procedures could be find in the work of Tagoe *et al* [1]. These measurements were done to account for variations in scatter contribution to dose at any point within a phantom/ patient for using a compensator to represent the bolus. Effect of beam hardening was ignored as it was considered minimal for cobalt 60 beam. Once the physical dimensions of a compensator were determined through the above procedures, the compensator was constructed using the cubic pile approach [14].

To account for beam divergence, a compensator sheet with grid lines (beamlet) having dimensions of 1 cm x 1 cm was developed for recording bolus/compensator material thickness across a radiation field. The compensator sheet had two bolded broken lines running central to the sheet, which were used to represent the major axes of a beam. The equivalent dimensions of a grid on the sheet at the teletherapy machine isocenter was determined to facilitate the realization of the area covered by an applied bolus on the surface of the phantom per grid (or beamlet) relative to the isocentre. A compensator was constructed by stacking and piling blocks (having dimensions of 1 cm x 1 cm) of the required compensator material to obtain compensator material thicknesses indicated on the compensator sheet. The output of a constructed compensator was verified with the Gafchromic EBT2 film.

To facilitate the use of the Gafchromic EBT2 film as a dosimeter, strips of the film were irradiated to known doses (calculated from measured beam output of the telecobalt machine) to obtain sensitometric curve for the film. Beam output calibration of the telecobalt machine to facilitate the usage of the radiochromic film for dosimetry was done with the 0.6 cc Farmer type ionization chamber inserted into the stationary water phantom, using the IAEA TRS 398 protocol [8]. During the output measurement, the 0.6 cc ionization chamber was connected to the UNIDOS electrometer. The equation of the line of best fit of the sensitometric curve was used for converting optical densities of film to doses. The overall accuracy of EBT2 film measurements was derived using the method proposed by van Battum *et al*. [15], that took into account the most pronounced sources of uncertainties in dose determination (scanner, lateral correction, fit accuracy, intra-batch variation, background, intrinsic film inhomogeneity), and using error propagation analysis an overall uncertainty of less than or equal to 2.0% was observed. The beam output calibration of the telecobalt machine was found to have an associated overall uncertainty of 1.4%. This gave the film dosimetry an overall uncertainty of less than or equal to 2.6%.

To verify Outputs of the proposed approach, a number of treatment plans using a single field with varying irradiation geometries were created for the solid dry phantom. Bolus in the form of step wedges placed on the surface of the solid phantom at the point of beam entrance were used to provide intensity modulation of beams. For each created bolus, the bolus was assigned a density similar to that of water (HU=0), which was the default for the TPS. Two types of step wedges were created for the assessment. The wedges mounted on the solid phantom are depicted in transverse view of the main planning windows shown in **Figure 3**. The created treatment plans were each replicated on the telecobalt machine with a bolus within the radiation field represented with a compensator constructed using the cubic pile approach, such that the thickness of the compensator along the direction of propagation of the beam at any portion of the radiation field determined using **Equation 2**. Compensators were constructed from each of the selected

compensator materials per treatment plan for the verification. A constructed compensator was mounted on a block tray similar to what is used in the department for mounting of customized shielding blocks, and held on the accessory holder of the teletherapy machine. A compensator was aligned such that its height was towards the radiation source. For each irradiation with a compensator, it was ensured that the block tray was at least 15 cm from the surface of the phantom to minimize electron contamination and also to prevent the compensator from acting as a beam spoiler [16]. Treatment plans were grouped into two case scenarios: case scenario 1 for irradiation geometries having the step wedge depicted in **Figure 3A**, and those with the step wedge shown in **Figure 3B** were considered as case scenario 2. Dose distributions within the phantom along the depth of dose prescription for the various treatment plans were assessed with the Gafchromic films from the same batch, and compared to those calculated with the TPS having boluses. For the film irradiations, the film strips were sandwiched between acrylic slabs of the solid dry phantom at the required depth and held on the treatment couch of the teletherapy machine under gravity. All exposed films used in this study were scanned with the ScanMaker 9800XL plus flatbed scanner, and images obtained (saved in Tagged Image File Format) analyzed with an ImageJ software (National Institutes of Health, USA) to obtain optical densities of films. The optical density of exposed film under a compensator was converted to dose using the equation of the line of best fit of the sensitometric curve obtained for the Gafchromic film.

The difference between the measured and the calculated doses, δ(%), was defined as following:

$$\delta(\%) = 100 \times (D_{calc.} - D_{meas.})/D_{meas.} \quad \text{Eq. 3}$$

where $D_{calc.}$ and $D_{meas.}$ are the calculated dose by TPS and the measured dose with film, respectively. The overall confidence limit for the proposed approach, Δ, was therefore defined as:

$$\Delta = |Average\ deviation| + 1.5 \times SD \quad \text{Eq. 4}$$

To accomplish the dose assessment, at the depth of dose prescription for each plan, calculation points 2 cm apart from each other were placed along a major axis of a beam to cover the entire field. The major axis was chosen such that it ran across steps of a step wedge. The boluses were created such that a step ran central to a calculation point. Calculation points were the dose determination point within the phantom occurred outside a step was not accounted. Our primary concern was not on the resolution of the dose distributions within the phantom, but the magnitude of doses within the phantom for a particular calculation point. The shape of a bolus resulted in the creation of varying doses at the various calculation points, due to varying beam attenuation achieved with the different thicknesses of the various steps of a step wedge bolus.

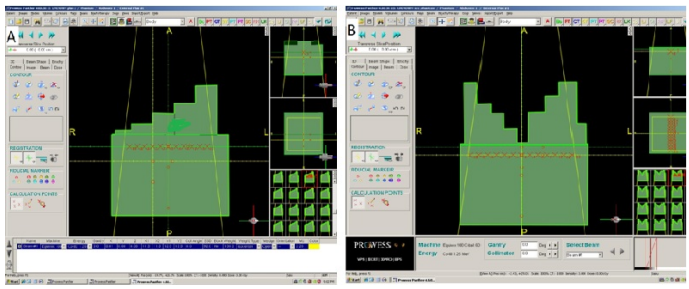

Figure 3. Planning windows showing axial configuration of bolus used for assessment of proposed approach.

Table 1. Measured radiological properties of selected compensator materials and water.

Material	Density (g/cm^3)	Mass attenuation coefficient (cm^2/g)	Relative mass attenuation coefficient (relative to that of water)
Water	1.0000±0.0100	0.0678	1.0000
Perspex	1.1800 ±0.0100	0.0697	1.0287
Brass	8.5500±0.0500	0.0597	0.8798
Copper	8.9400 ±0.0200	0.0570	0.8409

Table 2. Expressions for terms in function for converting bolus thickness to compensator material thickness.

Compensator material	Thickness Ratio, T	Field size correction factor, f_r	Treatment depth correction factor, f_d
Perspex (PMMA)	$(-5.0\times10^{-7})t_b{}^5 + (3.0\times10^{-5})t_b{}^4 - (6.0\times10^{-4})t_b{}^3 + (4.6\times10^{-3})t_b{}^2 + (3.1\times10^{-3})t_b + (517.4\times10^{-3})$	$(-3.0\times10^{-8})r^6 + (4.0\times10^{-6})r^5 - (2.0\times10^{-4})r^4 + (4.2\times10^{-3})r^3 - (48.3\times10^{-3})r^2 + (234.2\times10^{-3})r + (782.1\times10^{-3})$	$(6.0\times10^{-7})d^5 - (3.0\times10^{-5})d^4 + (8.0\times10^{-4})d^3 - (12.7\times10^{-3})d^2 + (89.7\times10^{-3})d + (783.5\times10^{-3})$
Copper	$(-5.0\times10^{-8})t_b{}^5 + (2.0\times10^{-6})t_b{}^4 - (3.0\times10^{-5})t_b{}^3 + (8.0\times10^{-5})t_b{}^2 + (4.7\times10^{-3})t_b + (7.1\times10^{-2})$	$(-1.0\times10^{-8})r^6 + (2.0\times10^{-6})r^5 - (9.0\times10^{-5})r^4 + (2.2\times10^{-3})r^3 - (26.8\times10^{-3})r^2 + (130.4\times10^{-3})r + (907.4\times10^{-3})$	$(9.0\times10^{-7})d^5 - (4.0\times10^{-5})d^4 + (7.0\times10^{-4})d^3 - (7.7\times10^{-3})d^2 + (53.6\times10^{-3})d + (86.4\times10^{-2})$
Brass	$(-4.0\times10^{-8})t_b{}^5 + (2.0\times10^{-6})t_b{}^4 - (5.0\times10^{-5})t_b{}^3 + (6.0\times10^{-4})t_b{}^2 + (2.0\times10^{-3})t_b + (100.4\times10^{-3})$	$(-3.0\times10^{-8})r^6 + (3.0\times10^{-6})r^5 - (2.0\times10^{-4})r^4 + (3.4\times10^{-3})r^3 - (3.9\times10^{-2})r^2 + (183.2\times10^{-3})r + (861.9\times10^{-3})$	$(-3.0\times10^{-6})d^5 + (1.0\times10^{-4})d^4 - (1.2\times10^{-3})d^3 + (1.2\times10^{-3})d^2 + (49.8\times10^{-3})d + (810.4\times10^{-3})$

Table 3. Calculated and measured doses at the various calculation points for compensators constructed from the selected materials per case scenario.

Plan #	Calc. Pt #	Calc. dose (cGy)		Meas. doses (cGy)					
				Perspex		Brass		Copper	
		Case 1	Case 2	Case 1	Case 2	Case 1	Case 2	Case 1	Case 2
	1	100.00	100.00	100.00	101.01	102.38	101.03	100.50	101.78
	2	98.38	85.08	99.57	87.07	96.87	83.77	100.70	87.05
1	3	92.06	80.29	94.03	78.29	89.92	78.42	93.50	78.84
	4	86.56	69.38	85.51	70.70	89.22	71.51	88.04	71.29
	5	82.54	66.79	84.52	68.39	84.66	68.50	82.08	65.12
	1	150.00	150.00	151.32	152.86	154.10	152.53	154.64	151.29
	2	148.15	125.75	152.73	128.15	152.73	128.64	152.56	129.24
	3	146.37	123.47	150.22	125.72	147.37	126.87	150.05	126.44
2	4	129.54	99.70	131.46	101.38	130.82	101.92	133.11	101.69
	5	126.30	98.48	128.33	100.16	130.06	101.15	128.60	101.09
	6	159.70	94.90	164.10	96.82	162.71	97.70	162.71	97.19
	7	121.30	94.80	123.84	97.18	124.88	96.71	125.03	97.71
	1	200.00	200.00	198.57	203.50	203.05	203.05	204.08	202.00
	2	198.17	169.79	203.48	165.86	202.52	174.27	202.67	174.97
	3	196.67	170.48	202.07	175.16	192.21	174.53	201.63	175.01
	4	175.36	140.83	173.66	145.16	170.25	137.73	177.22	144.99
	5	174.27	139.99	177.97	142.91	179.59	135.91	176.44	143.18
	6	220.14	140.00	222.43	141.46	226.04	143.80	226.69	144.17
3	7	173.48	138.45	177.49	141.94	177.87	142.67	178.44	142.41
	8	214.61	136.12	220.11	138.83	220.00	139.58	220.43	139.81
	9	167.95	117.51	165.01	119.52	172.01	120.82	172.40	120.80
	10	206.83	110.05	211.22	112.73	212.94	113.27	212.50	112.28
	11	208.25	110.82	213.11	113.41	212.67	113.99	213.90	113.01
	12	130.61	107.56	132.20	105.60	134.47	110.85	134.65	110.31
	13	123.53	58.01	126.05	59.79	127.35	59.80	127.32	59.79
	1	250.00	250.00	252.53	253.96	254.84	254.84	256.41	253.81
	2	248.60	213.25	255.76	207.44	252.85	219.12	252.49	219.82
	3	246.85	214.02	243.32	210.96	253.91	208.96	251.55	220.30
	4	222.63	176.95	228.34	181.60	229.23	182.22	219.21	172.37
	5	220.48	176.70	226.60	181.75	226.11	181.58	215.86	172.90
	6	277.75	175.81	286.34	178.22	285.16	180.80	285.22	171.32
4	7	219.26	173.65	223.55	177.05	223.96	178.01	223.46	178.98
	8	270.00	171.55	276.07	175.41	277.24	176.35	274.31	176.29
	9	212.27	148.02	216.51	150.37	215.59	151.91	218.14	152.11
	10	259.69	138.92	265.23	136.00	265.40	142.48	267.01	143.13
	11	263.04	139.88	260.44	142.73	270.28	135.81	270.26	143.72
	12	167.20	135.44	168.70	138.05	170.70	139.27	171.80	139.17
	13	158.14	122.27	162.19	125.92	162.96	126.05	162.83	125.77
	1	250.00	250.00	252.47	253.24	257.73	254.01	255.39	253.96
	2	247.82	227.48	253.65	232.98	255.43	233.36	253.50	233.94
	3	247.62	226.01	254.18	230.55	253.03	231.90	254.99	231.73
	4	225.60	195.12	227.63	198.82	231.79	200.78	231.62	200.66
	5	224.56	194.58	231.51	198.33	230.32	199.63	230.91	200.29
	6	266.20	194.76	263.43	190.57	272.19	200.00	273.53	200.33
5	7	221.67	192.11	227.77	195.99	228.53	197.20	227.70	197.14
	8	261.36	192.08	269.44	195.50	266.64	197.98	269.14	198.00
	9	185.29	171.04	189.94	176.06	189.98	176.08	190.00	175.75
	10	251.41	140.66	255.47	145.01	257.80	144.24	258.36	144.62
	11		161.59		165.99		165.39		156.88
	12	174.62	157.61	176.38	160.29	179.10	161.65	180.02	162.45
	13		116.81		119.06		120.29		120.42

Table 4. Comparison between measured doses with compensators and TPS calculated doses with boluses.

Plan #	Calc. Pt #	Percentage Diff. between Calc. and Meas. doses (%)					
		Perspex		Brass		Copper	
		Case 1	Case 2	Case 1	Case 2	Case 1	Case 2
	1	0.00	1.00	2.32	1.02	0.50	1.75
	2	1.20	2.28	-1.56	-1.56	2.30	2.26
1	3	2.10	-2.56	-2.38	-2.38	1.54	-1.84
	4	-1.23	1.87	2.98	2.98	1.68	2.68
	5	2.34	2.34	2.50	2.50	-0.56	-2.56
	1	0.87	1.87	2.66	1.66	3.00	0.85
	2	3.00	1.87	3.00	2.25	2.89	2.70
	3	2.56	1.79	0.68	2.68	2.45	2.35
2	4	1.46	1.66	0.98	2.18	2.68	1.96
	5	1.58	1.68	2.89	2.64	1.79	2.58
	6	2.68	1.98	1.85	2.87	1.85	2.36
	7	2.05	2.45	2.87	1.97	2.98	2.98
	1	-0.72	1.72	1.50	1.50	2.00	0.99
	2	2.61	-2.37	2.15	2.57	2.22	2.96
	3	2.67	2.67	-2.32	2.32	2.46	2.59
	4	-0.98	2.98	-3.00	-2.25	1.05	2.87
	5	2.08	2.04	2.96	-3.00	1.23	2.23
	6	1.03	1.03	2.61	2.64	2.89	2.89
3	7	2.26	2.46	2.47	2.96	2.78	2.78
	8	2.50	1.95	2.45	2.48	2.64	2.64
	9	-1.78	1.68	2.36	2.74	2.58	2.72
	10	2.08	2.38	2.87	2.84	2.67	1.99
	11	2.28	2.28	2.08	2.78	2.64	1.94
	12	1.20	-1.86	2.87	2.97	3.00	2.49
	13	2.00	2.98	3.00	3.00	2.98	2.98
	1	1.00	1.56	1.90	1.90	2.50	1.50
	2	2.80	-2.80	1.68	2.68	1.54	2.99
	3	-1.45	-1.45	2.78	-2.42	1.87	2.85
	4	2.50	2.56	2.88	2.89	-1.56	-2.66
	5	2.70	2.78	2.49	2.69	-2.14	-2.20
	6	3.00	1.35	2.60	2.76	2.62	-2.62
4	7	1.92	1.92	2.10	2.45	1.88	2.98
	8	2.20	2.20	2.61	2.72	1.57	2.69
	9	1.96	1.56	1.54	2.56	2.69	2.69
	10	2.09	-2.15	2.15	2.50	2.74	2.94
	11	-1.00	2.00	2.68	-3.00	2.67	2.67
	12	0.89	1.89	2.05	2.75	2.68	2.68
	13	2.50	2.90	2.96	3.00	2.88	2.78
	1	0.98	1.28	3.00	1.58	2.11	1.56
	2	2.30	2.36	2.98	2.52	2.24	2.76
	3	2.58	1.97	2.14	2.54	2.89	2.47
	4	0.89	1.86	2.67	2.82	2.60	2.76
	5	3.00	1.89	2.50	2.53	2.75	2.85
	6	-1.05	-2.20	2.20	2.62	2.68	2.78
5	7	2.68	1.98	3.00	2.58	2.65	2.55
	8	3.00	1.75	1.98	2.98	2.89	2.99
	9	2.45	2.85	2.47	2.86	2.48	2.68
	10	1.59	3.00	2.48	2.48	2.69	2.74
	11		2.65		2.30		-3.00
	12	1.00	1.67	2.50	2.50	3.00	2.98
	13		1.89		2.89	0.50	3.00

Results

In **Table 1** are listed measured radiological properties of the various compensator materials used in the study including those of water. Densities and mass attenuation coefficients are provided for the selected materials earmarked for compensator construction. Also presented in **Table 1** are ratios of mass attenuation coefficient of a compensator material to that of water for the respective compensator materials. Determined expressions for the various terms in **Equation 2** through the correlation analyses using the lines of best fits and regressions, R^2 are listed in **Table 2**. Where the various terms: t_b, r and d within the expressions listed in **Table 2** are applied bolus thickness during treatment planning with the TPS in cm, equivalent square field size of the actual field size used, and treatment depth in cm, respectively. In **Table 3** are listed doses calculated (calc. dose) at the various calculation points (calc. Pt. #) obtained with the TPS having boluses within the radiation fields and their measured counterpart with the boluses represented with compensators constructed based on the proposed approach, when the generated treatment plans were replicated on the telecobalt. The percentage differences between the calculated and measured doses for the various calculation points for compensators constructed from the selected materials are enumerated in **Table 4**. The various dose differences are each expressed as a percentage of the respective measured doses, and are calculated using **Equation 3**.

Discussions

Prior to the use of the proposed approach, it is imperative to determine the radiological properties of the material one wants to use for the construction of a compensator. Changes in the elemental composition of a material may have significant influence on the expressions determined for the various terms in the semi-empirical equation proposed for the conversion of a bolus thickness to a compensator material thickness. This is because all the measurements acquired to ensure the development of the expressions for the various terms in the semi-empirical equation were based on transmission measurements with a compensator material in the path of the beam. The most reliable quantity to determine for the material is the mass attenuation coefficient measured with the same beam quality as that to be modulated. It is also verifiable that changes of elemental composition and or impurities within constituent elements of a material would affect the value of attenuation coefficient measured for the material with a particular beam quality [17]. Owing to uncertainties in the experimental setup for the measurement of the attenuation coefficient, it would be prudent for one to normalize the attenuation coefficient of a material to that of water measured with the same irradiation geometry. The normalized attenuation coefficient which is referred to as relative mass attenuation coefficient in **Table 1**, should be used to characterize a material prior to the use of the proposed approach. Also, one needs to be circumspective with the use of the proposed approach even when the attenuation coefficient of a material is comparable to what is presented in **Table 1**; as the various expressions determined for the conversion of a bolus thickness to compensator material thickness may be dependent on design of collimator system of a teletherapy machine. The expressions must therefore be determined for ones teletherapy machine. In determining the expressions for the various terms in the proposed semi-empirical equation for converting bolus thickness to compensator material thickness, one needs to incorporate ranges of treatment parameters (field size, treatment depth and applied bolus thickness) that are likely to be used clinically during the experimental measurements. Ignoring this will lead to uncertainties in the dose distribution obtained with a compensator; owing to the degrees of the polynomial equations which are used to express the various terms of the semi-empirical equation presented in **Table 2**. From the dose comparison results in **Table 3**, it shows that none of compensator materials can be favoured over the other for the construction of a compensator.

The choice of a compensator material is therefore dependent on convenience with which the compensator can be constructed with a particular material and the level of beam intensity modulations required. Where high levels of modulations are required, the compensator should be constructed from materials with higher density values or lower relative mass attenuation values. This will minimize the thickness of a constructed compensator, thereby reducing the magnitude of penumbra associated with the beam resulting from the introduction of the compensator in the path of the beam. With reference to the dose comparison results in **Table 3**, compensators constructed from Perspex give the most comparable doses to those of the TPS, which may be attributed to the closeness of the radiological properties of Perspex to those of water. This also goes to support the point that using medium density materials for compensator constructing would translate to low discrepancies in dose distributions obtained with a compensator for uncertainties in the determination of thickness of the compensator.

Although the proposed approach gave favourable results, the following limitations were encountered: bolus thickness could not be increased beyond 15 cm and for abutting fields, bolus could not be entered for individual field. These were inherent limitations associated with the TPS used.

Owing to the inherent uncertainties associated with the film dosimetry, there is the need to further study the output of proposed approach with other 2D array detector based on diode or ionization chamber. Notwithstanding this, the output of the proposed approach is within the ± 5% uncertainty proposed for dose delivery in radiation therapy [18]. Also, one needs to institute some form of quality assurance procedures to ensure effective implementation of the proposed approach. The proposed approach may be used to enhance spatial resolution of dose distribution within irradiated regions having high levels of tissue heterogeneities (eg. treatment of lung cancers) and tissue deficiencies (eg. treatment of head and neck cancers).

Conclusion

A pilot study using quasi-experimental approach had been conducted, to propose and develop an approach of generating intensity modulated beams for a conventional telecobalt machine with compensating filters, based on generated dose distributions of a forward planning TPS (with limitations of realizing beam intensity maps). It had been shown that, it is practically possible to generate modulated fluence distributions across beams from the telecobalt machine using bolus having varying thicknesses across the surface of a phantom (or patient) during treatment simulation with the forward planning TPS, and then replicating the treatment with a compensator at the time of treatment delivery. A proposed semi-empirical equation has been found to be effective in converting bolus thickness to compensator material thickness such that the dose distribution within the phantom (or patient) remains the same as planned with the TPS. Terms within the proposed equation to account for effects of treatment parameters, have been established for Brass, Copper and Perspex (PMMA), which were used as compensator materials. Dose distributions measured under a compensator (fabricated based on the proposed approach) in a tissue-equivalent phantom with calibrated radiochromic films, are found to compare favourably well to those of the TPS (where bolus was used to provide beam intensity modulations). Radiological properties are provided for the stipulated compensator materials to ensure reproducibility of the proposed approach.

Acknowledgements

This publication formed part of research work carried out by the principle author to enable him complete his PhD thesis, which was submitted to the Department of Physics, School of Physical Sciences, College of Agriculture and Natural Sciences, University of Cape Coast, Ghana, in partial fulfillment of a PhD degree.

References

[1] Tagoe SNA, Mensah SY, Fletcher JJ, Sasu E. Telecobalt Machine Beam Intensity Modulation with Aluminium Compensating Filter Using Missing Tissue Approach. Iraj J Med Phys. 2018;15(1):48-61 .

[2] Schlegel W, Bortfeld T, Grosu A. New technologies in radiation oncology. Springer-Verlag Berlin Heidelberg, Germany. 2006.

[3] Khan FM. The physics of radiation therapy. Fourth Edition. Lippincott William and Wilkins. 2010.

[4] Vaarkamp J, Adams EJ, Warrington AP, Dearnaley DP. A comparison of forward and inverse planned conformal, multi segment and intensity modulated radiotherapy for the treatment of prostate and pelvic nodes. Radiother Oncol. 2004;73(1):65-72.

[5] Shepard DM, Earl MA, Li XA, *et al*. Direct aperture optimization: A turnkey solution for step-and-shoot IMRT. Med Phys. 2002:29(6): 1007-1018.

[6] Van de Werf E, Verstraete J, Lievens Y. The cost of radiotherapy in a decade of technology evolution. Radiother Oncol. 2012;102(1): 148-153.

[7] Chang S. Compensating filter-intensity-modulated Radiotherapy – A Traditional Tool for Modern Application. European Oncological Disease. 2006;1(2):82-87.

[8] International Atomic Energy Agency (IAEA). Technical report series 398. Absorbed dose determination in external beam radiotherapy. IAEA. 2000.

[9] Podgorsak EB. Radiation oncology physics: A handbook for teachers and students. International Atomic Energy Agency (IAEA). 2005.

[10] Canadian Nuclear Safety Commission. Certified Transport Packages and Special Form Radioactive Material. Canadian Nuclear Safety Commission. 2012.

[11] Nelms B, Markman J. Implementation of 'solid IMRT': modulator design, fabrication, dose delivery, and quality assurance. Australas Phys Eng Sci Med. 2001;24(4):223-224.

[12] Prowess Inc. Prowess Panther treatment planning system user manual. Prowess Inc., USA. 2003.

[13] Earl MA, Afghan MKN, Yu CX, *et al*. Jaws-only IMRT using direct aperture optimization. Med Phys. 2007:34(1):307-314.

[14] Sasaki K, Obata Y. Dosimetric characteristics of a cubic-block-piled compensator for intensity-modulated radiation therapy in the Pinnacle radiotherapy treatment planning system. J Appl Clin Med Phys. 2007;8(1):85-100.

[15] van Battum LJ, Hoffmans D, Piersma H, Heukelom S. Accurate dosimetry with GafChromic EBT film of a 6 MV photon beam in water: what level is achievable? Med Phys. 2008;35(2):704-716.

[16] Kassaee A, Bloch P, Yorke E, *et al*. Beam spoilers versus bolus for 6 MV photon treatment of head and neck cancers. Med Dosim. 2000;25(3):127-131.

[17] Amin NAB, Zukhi J, Kabir NA, Zainon R. Determination of effective atomic numbers from mass attenuation coefficients of tissue-equivalent materials in the energy range 60 keV- 1.33 MeV. IOM Conf Series: Journal of Physics: Conference Series. 2017;851(1):012018.

[18] van der Merwe D, Van Dyk J, Healy B, *et al*. Accuracy requirements and uncertainties in radiotherapy: a report of the International Atomic Energy Agency. Acta Oncol. 2017;56(1):1-6.